



Article

Tailoring the Properties of Ni(111)/Graphone Interfaces by Intercalation of Al and Na: A DFT Study

Ramakrishnan Archana, Niharika Joshi and Thirumalaiswamy Raja *

CSIR-National Chemical Laboratory, Catalysis and Inorganic Chemistry Division,
Pune 411008, Maharashtra, India

* Correspondence: t.raja@ncl.res.in; Tel.: +91-20-2590-2006

Abstract: With the incredible discovery of graphene (Gr), all of the properties studied to date suggest that it has promising applications in the development of semiconductor, spintronic, insulating, and polymer materials. However, efforts are still underway to fully understand the nature of metal–graphone(GrH) interaction in order to offer better scope for tuning the electronic and magnetic properties, which can be performed by intercalation of atoms via metal support on graphene. We chose metal atoms belonging to the s and p blocks, namely Na and Al, respectively, as the intercalating atoms. Herein, the maximum coverage of a monolayer of Na and Al was comparatively studied on a Ni(111) surface. Significant changes in the magnetic and electronic properties at the Ni(111)/graphone interface were observed upon intercalation. Of the two intercalating metal atoms, Na proved to be more effective, such that the magnetic properties of the surface Ni were only slightly decreased, and the graphone also showed better magnetic properties than in the absence of Na.

Keywords: graphone; Ni(111)/graphone interface; intercalation; spintronic



Citation: Archana, R.; Joshi, N.; Raja, T. Tailoring the Properties of Ni(111)/Graphone Interfaces by Intercalation of Al and Na: A DFT Study. *C* **2022**, *8*, 62. <https://doi.org/10.3390/c8040062>

Academic Editors: Jin-Hae Chang and Marcelo Antunes

Received: 25 September 2022

Accepted: 19 October 2022

Published: 9 November 2022

Publisher's Note: MDPI stays neutral with regard to jurisdictional claims in published maps and institutional affiliations.



Copyright: © 2022 by the authors. Licensee MDPI, Basel, Switzerland. This article is an open access article distributed under the terms and conditions of the Creative Commons Attribution (CC BY) license (<https://creativecommons.org/licenses/by/4.0/>).

1. Introduction

Due to the remarkable properties of graphene [1], it has attracted attention from the inquisitive minds of several researchers, who have explored graphene in both experimental and theoretical studies. The functionalization and dispersion of graphene sheets are crucial to their end applications [2–4]. Sofo and co-workers transformed semi-metallic materials into insulators upon complete hydrogenation of graphene (graphane), making it possible to modify the band gap properties [5]. The band gap opening can be appropriately tuned in 2D materials by means of chemical derivatization, which was studied in graphene, specifically, by Vladimir V. Shnitov et al. [6]. Spectacular research has been performed both experimentally and theoretically on the functionalization of graphene with hydrogen [7,8]. Graphene functionalized by semi-hydrogenation is known as graphone; the functionalization breaks the delocalized π bonding, resulting in a small indirect band gap. At the same time, the electrons on the unhydrogenated carbon atoms become unpaired and localized, giving rise to a magnetic moment of $1.0 \mu_B$, resulting in the material becoming a ferromagnetic semiconductor [9]. For this reason, tuning graphene by means of hydrogenation is gaining popularity due to its distinctive properties and applications. However, the imbalance in the sublattice results in instability in free-standing graphone, which mainly arises due to the fact that carbon atoms of only one of the sublattice sheets of graphene is adsorbed by hydrogen [10]. This has prompted researchers to study hydrogen adsorption with various degrees of coverage in order to better understand the optimization of the magnetic and electronic properties for the purposes of hydrogen storage applications [11–13]. This instability can be overcome through stabilization using transition metal surfaces, as studied by Zhao et al. [14]. Such materials find promising and novel applications in graphene-based semiconductors and spintronic devices. The transition metal surfaces were chosen based on their—lattice parameters close to those of graphene. The surfaces were studied either

by physisorption (Ir, Pt, Au, Cu) or chemisorption (Co, Ni, Ru, Pd) on epitaxial graphene. The electronic structure of graphene is strongly perturbed by chemisorption, while it is essentially preserved in the weak binding “physisorption” regime [15].

Various studies on the intercalation of atoms have been performed computationally, and many reports have also been experimentally validated using techniques like LEED, ARPES, STM, NEXAFS, and AES. Surfaces like Ir [16], Ru [15], Ni and Co [17] have been used in the study of graphene adsorption. The affinity of graphene to the substrate is such that it results in a strong interaction between the graphene and the substrate. Thus, to retain the properties of graphene, P. Sutter et al. [15], described a method for tuning the coupling of graphene onto the substrate by establishing routes via the intercalation of metals. Intercalation of alkali metals can lead to a significant increase in graphene/substrate separation, decoupling the graphene from the substrate, accompanied by a recovery of the dispersion of the π band. Studies have included a broad class of elements, ranging from alkali metals and transition metals to a few lanthanide elements and amongst the alkali metals, Li has the strongest affinity for intercalation against adsorption, resulting in an energy difference of around 1 eV [18].

It was also found by M. Weser and coworkers [19] that the intercalation of Fe between graphene and Ni(111) results in some changes in the magnetic response from the graphene layer. In the case of the intercalation of transition and noble metals, spin scattering may appear in the graphene-based spin filters due to the d-orbitals [19,20], and the d-d orbital interaction may result in strong binding and affinity between the substrate and the intercalated atom, giving rise to a strong chemical interaction. Similarly, Joshi N et al. demonstrated enhanced magnetic moments in oxygen with intercalation of graphene [21]. However, oxygen may not remain inert under atmospheric conditions, and may undergo further oxidation. Analyzing the properties of intercalated atoms on a comparative basis, the proposed study is based on the intercalation of atoms belonging to elements of the s and p blocks. This comparative study is performed by undertaking intercalation with monolayers of Al and Na atoms, occupying the maximum coverage with respect to the lattice parameter(s) of the Ni(111) surface. Improved magnetic properties at the interface between Ni(111) and graphene were observed when intercalation was performed with Na, indicating Na to be a more efficient atom for intercalation than Al. As a result of the properties of Na, such materials will have better applications in the production of cost-effective semiconductors.

The remainder (remaining) of this paper is organized as follows: in the section below, the methodology of the work is described, and the computational details are elaborated. The next section includes the detailed results of our investigation, as well as a discussion. Lastly, a conclusion is provided in which the work is summarized, and further scope for studies on this system are noted.

2. Materials and Methods

We performed ab initio calculations on the basis of density functional theory (DFT) using Quantum Espresso Software in the current computational study involving a plane-wave basis set [22]. We used the ultrasoft pseudopotentials to solve the electron-ion interactions [23]. The kinetic energy cutoffs for the wavefunction were set to 35 Ry, while the charge density was set to 360 Ry. The electron–electron exchange–correlation potential was described using Perdew, Burke, and Ernzerhof’s parametrization of the generalized gradient approximation (GGA) [24]. Brillouin zone integrations were performed on a $16 \times 16 \times 1$ shifted Monkhorst Pack k-point grid per (1×1) Ni(111) surface unit cell [25]. In order to efficiently speed up the calculations to achieve convergence, we used Marzari–Vanderbilt smearing with a width of 0.005 Ry [26].

Our model for the present investigations of the intercalating system consists of an asymmetric slab consisting of 6 layers of Ni(111) surface. Fixing the bottom 3 layers at the bulk interplanar distance (2.03 Å), relaxation of the top 3 layers was carried out. A vacuum of 15 Å was used to ensure that the interactions were minimized in the periodic images

perpendicular to the surface. In order to test the pseudopotentials, the lattice parameter and magnetic moment of bulk Ni, the lattice parameters, corresponding to the bond length, of Al, Na, and C and C-C in free-standing graphene were computed. The obtained results for the lattice parameter and magnetic moment for bulk Ni were found to be 3.52 Å and 0.64 μ_B per Ni atom, respectively. In addition, the lattice parameters of Al and Na were 4.047 and 4.29 Å, respectively. It was observed that for freestanding graphene, the lattice parameter was 2.46 Å, having a C-C bond length of 1.43 Å. The results mentioned above are in agreement with those presented in previously published reports [27].

To better understand the interaction of the intercalated atom and the carbon atoms of the graphene/graphone sheets, which ultimately affects the C-H bond strength in graphone, the resulting binding energies were computed and calculated as follows:

$$E_b = E_{\text{substrate/adsorbate}} - E_{\text{adsorbate}}$$

where substrate = Ni(111) or Ni(111)/Al or Ni(111)/Na and adsorbate = Gr or Gr/H.

3. Results

Before discussing the results obtained for graphone adsorbed on the modified Ni(111) surface, the results for the modified Ni(111) surface alone will be discussed, as well as the adsorption of graphene on the modified Ni(111) surface. As mentioned above, we modified the Ni(111) surface by covering its top layer with Al and Na metal atoms.

3.1. Modified Ni(111) Surface

For the purposes of our study, we chose the most extensive possible coverage of Al atoms, which is 0.75 Monolayer (ML). We modeled this coverage by taking 2×2 unit cells of Ni(111). Thus, there are 3 Al atoms, corresponding to four surface Ni atoms. The Al-Al distance at this coverage is around 2.80 Å, which is equal to the lattice parameter of the Al(111) surface. Figure 1a presents the top view of the Ni(111) surface covered with Al atoms (Ni(111)/Al) at 0.75 ML coverage. It can be observed that the Al atoms occupy all three available adsorption sites on the Ni(111) surface, namely top, hcp, and fcc. Thus, at a coverage of 0.75 ML, there is just one possible arrangement of the Al atom on the Ni(111) surface. Figure 1b also shows the side view of the Ni(111)/Al surface. We observed that both the top Ni(111) layer and Al layer are buckled. The buckling in the Al layer is around 0.26 Å, while that in the top Ni(111) layer is about 0.09 Å. The buckling arises due to the direct interaction of Al at the top site (Al^{top}) with one of the surface Ni (Ni¹). As both Al and Ni are electropositive, the interaction is repulsive. Ni¹ is pushed down, while Al^{top} moves up, resulting in an Ni–Al distance of around 2.34 Å. The Ni–Al distance for Al in the hollow sites is about 2.45 Å.

Furthermore, we note from the Löwdin charge analysis that the Ni–Al interaction causes a decrease in the magnetic moments on the surface Ni atoms while on the surface Ni atoms in clean Ni(111) surface is 0.71 μ_B . The magnetic moment on Ni¹ is around 0.36 μ_B , while that on the rest of the surface Ni atoms (Ni⁰, Ni atoms with no direct interaction with Al atoms) is approximately 0.28 μ_B . To understand the difference in magnetic moments, we plotted the density of states of Ni-d of surface Ni and Al-p (Figure 2). It can be observed that the surface Ni is no longer half-metallic, as in the clean Ni(111) surface, and can be seen to conduct in both spin-channels. The otherwise-completely-filled Ni-d spin-up states increase their energy, exhibiting a finite number of states at Fermi energy. On the basis of Löwdin charge analysis, it can be found that Ni loses spin-up (gains spin-down) charge. However, the gain of spin-down charge (0.14 e by Ni⁰ and 0.12 e by Ni¹) is less than the amount of spin-up charge lost (0.24 e by Ni⁰ and 0.17 e by Ni¹). As a result, the magnetic moment for surface Ni is decreased. Moreover, due to the more repulsive interaction with Al, Ni¹ loses less charge than Ni⁰. This accounts for the improved magnetic moment on Ni¹ compared to on Ni⁰.

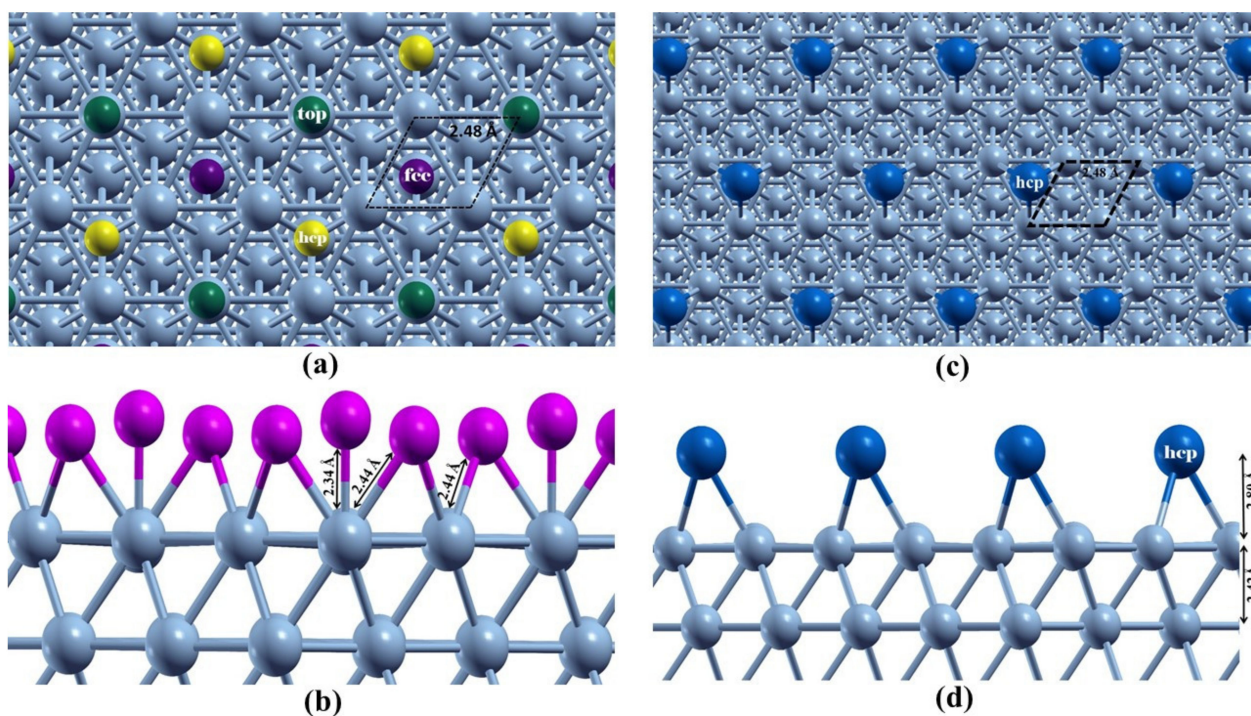


Figure 1. (a) Top view and (b) side view of Ni(111)/Al, where the grey atoms denote Ni, green, yellow, and purple denote the Al atoms at the top and the hollow sites of hcp and fcc, respectively; (b) the magenta atoms denote Al, (c) top and (d) side view of Ni(111)/Na, where the blue atoms denote Na at the hcp site.

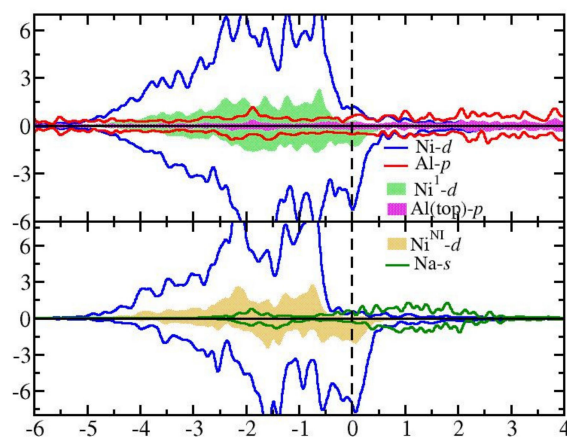


Figure 2. The upper panel presents the DOS plot for the Al intercalated system. Blue—the sum of all d states of Ni for all configurations. The red line is the sum of all p states of Al in Ni/Al. Light green shading—one of the Ni atoms interacting directly with Al^{top}, pink—Al^{top} interacting with the C (hydrogenated) of graphone. The lower panel presents the DOS plot for the Na intercalated system. Blue—the sum of d states of Ni in Ni/Na and the shaded region in yellow is the sum of all Ni-d states for the non-interacting surface Ni atom with Na. Green—s states of Na.

We performed our calculations for a coverage of Na of 0.25 ML, where there is a single Na atom for four surface Ni atoms. Therefore, we again modeled our system with a 2×2 unit cell of Ni(111) surface. The reason behind choosing such a low coverage for Na is as follows: The lattice parameter of Na(111) is around 3.72 Å. Therefore, the maximum coverage of Na will be less than 0.5 ML. Park et al. [27] considered different coverages ranging from 0.06 ML (0.16 ML, by their definition) to 0.42 ML (1.07 ML, by their definition).

However, they found that the effect of intercalation of Na on graphene becomes saturated after 0.25 ML (0.63 ML, by their definition).

At a coverage of 0.25 ML, the Na–Na distance is around 4.98 Å. We found that Na prefers to occupy either of the hollow sites. Figure 1c,d show the top and side view of the Ni(111) surface covered with Na atoms at a coverage of 0.25 ML (Ni(111)/Na), where Na takes the hcp site. Sodium at the hollow site interacts with three out of four surface Ni atoms. Consequently, it introduces a slight buckling of around 0.08 Å in the top Ni(111) layer. The Ni–Na distance is noted to be about 2.80 Å, which is more significant than the Ni–Al distance of 2.45 Å mentioned above for Al at the hcp (or fcc) site. Unlike for the Ni(111)/Al surface, we found that on the Ni(111)/Na surface, the magnetic moment on the surface Ni atoms shows just a small decrease compared to that on the clean Ni(111) surface. The magnetic moments on the three Ni atoms interacting with the Na atom is around 0.62 μ_B , while that on the remaining Ni atom is around 0.65 μ_B . Thus, from the geometry and magnetic moment values, we apprehend that the Ni–Na interaction is weaker than the Ni–Al interaction. This is also evident from the density of states plotted of Ni-d and Na-s in Figure 2, where negligible overlap between the Ni and Na states can be observed. Additionally, the DOS of Ni-d of Ni atoms interacting with Na (Ni(int)) and that of non-interacting Ni (Ni^{Ni}) atoms show only minor variations.

3.2. Graphene Adsorbed on Ni(111)/Al and Ni(111)/Na Surfaces

Next, the graphene sheet was adsorbed onto the Ni(111)/Al surface (Ni(111)/Al/Gr). Figure 3a shows the side view of Graphene adsorbed on Ni(111)/Al surface. We found a considerable distance of around 3.28 Å between the graphene and the Al-covered Ni(111) surface. As a result, the distances and geometry at the Ni(111)/Al surface remain more or less the same as those obtained before graphene adsorption. Therefore, the DOS of surface Ni-d and Al-p in Ni(111)/Al (Figure 2) and Ni(111)/Al/Gr (figure not included) are also observed to be similar. Hence, there is no notable change in the magnetic moments of the Ni atoms. The DOS of graphene adsorbed onto the Ni(111)/Al surface exhibits similar DOS to freestanding graphene, but only when the Dirac cone is shifted by 0.44 eV. Thus, graphene is only physisorbed onto the Ni(111)/Al surface. These results are in agreement with those reported by Voloshina et al. [28].

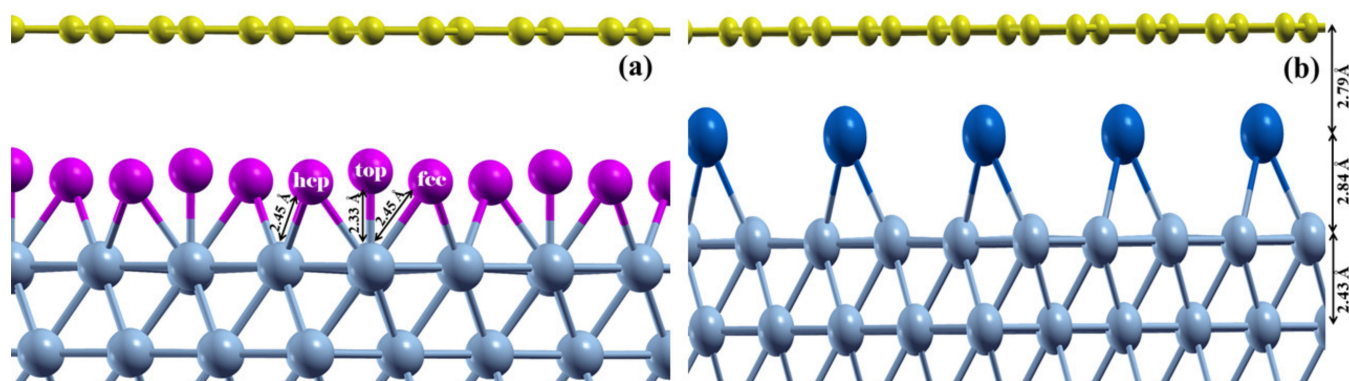


Figure 3. (a) Side view of Ni(111)/Al/Gr0.75 ML, the pink atoms represent Al, while the yellow atoms represent graphene sheet; (b) side view of Ni(111)/Na/Gr 0.25 ML, where blue atoms represent Na at the hcp site.

Upon adsorption of graphene on the Ni(111)/Na surface, we found that Na prefers to occupy the hcp site as represented in Figure 3b. The Ni(111)/Na/Gr with Na at the hcp site (Ni(111)/Na(hcp)/Gr) is lower in energy by 0.10 eV and 0.22 eV than the surface when Na is at the fcc and top sites, respectively. In Ni(111)/Na(hcp)/Gr, the Gr surface is observed to be around 2.40 Å (4.76 Å) away from the Na (top Ni(111)) layer, which is in perfect agreement with the distances reported by Park, et.al [27] for a coverage of 0.25 ML. The Na–C distance is around 2.79 Å. The Ni–Na bond distance increases slightly to 2.84 Å

from 2.80 Å, and the buckling in the top Ni(111) layer is decreased by 0.01 Å. Due to the low coverage of Na, some of the C atoms of the epitaxial graphene sheet do not interact with the intercalating Na atom. As a result, there is a tiny buckling of 0.01 Å in the graphene sheet.

The DOS plot for graphene adsorbed on Na-covered Ni(111) surface (Figure 4) shows that the Dirac cone is shifted to below the Fermi energy by 1.10 eV. This is, again, in good agreement with the results reported in [27]. Additionally, we find a mismatch between the spin-up and spin-down states of the p states of C of graphene in Ni(111)/Na(hcp)/Gr, implying a small induced magnetic moment on the graphene sheet. On the basis of Löwdin charge analysis, we find that a small magnetic moment of 0.01 μ_B is induced on the C of the graphene sheet, such that the orientations of the moments on C that interacts with Na are antiparallel with respect to those of C that does not interact with Na. Thus, the resultant magnetic moment on graphene is 0.04 per 2×2 unit cell. We also observed a significant magnetic moment of around 0.20 μ_B on the Na atom, aligned along the graphene's net magnetic moment. There is no change in the magnetic moment on Ni atoms after adsorption of the graphene sheet. However, the magnetic moments on the Ni are aligned antiparallel to the magnetic moments of Na and C atoms that interact with Na (parallel to C atoms that do not interact with Ni). The geometry, DOS, and magnetic properties of Ni(111)/Na/Gr suggest that there is a weak but significant interaction between the intercalating Na and Gr, unlike the interaction picture at the Ni(111)/Al/Gr interface.

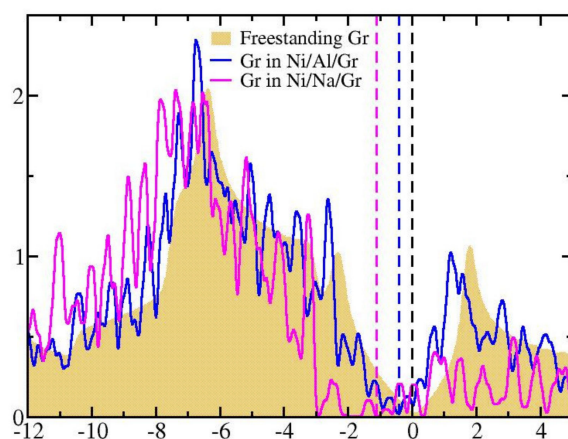


Figure 4. The shaded region in yellow is the DOS plot for pristine free-standing graphene, blue and pink lines denote graphene in Ni(111)/Al/Gr and Ni(111)/Na/Gr, respectively. The Dirac point shift was found by the lowest occupied density of states below the Fermi level (dotted vertical line).

3.3. Graphone on the Modified Ni(111) Surface

Graphone is adsorbed onto the Ni(111)/Al surface such that the hydrogenated (unhydrogenated) C takes the top (fcc) site. Since Al occupies all three adsorption sites on the Ni surface, there is one unhydrogenated and one hydrogenated C in the graphene sheet, which is placed right above the Al atom. Thus, within the sublattice formed by unhydrogenated C and hydrogenated C, there is a slight buckling of around 0.01 Å and 0.03 Å, respectively. The Al–C bond length, where the unhydrogenated C interacts directly with Al in the fcc site, is about 2.04 Å, as shown in Figure 5a, while the Al–C bond lengths between unhydrogenated C and Al in top and hcp sites are around 2.20 Å and 2.34 Å, respectively. The hydrogenated C at the top site moves away from the surface, but pushes the Al atom closer to the surface Ni such that the Ni–Al bond is around 2.24 Å. This bond length is smaller than that noted for the Ni(111)/Al surface, around 2.34 Å. The Al at hcp shows the weakest interaction with surface Ni, with a bond length of around 2.42 Å, which is close to the bond length observed before the adsorption of graphone (2.45 Å). The Al at fcc exhibits an intermediately strong interaction with surface Ni, with an Al–Ni bond length of around 2.30 Å.

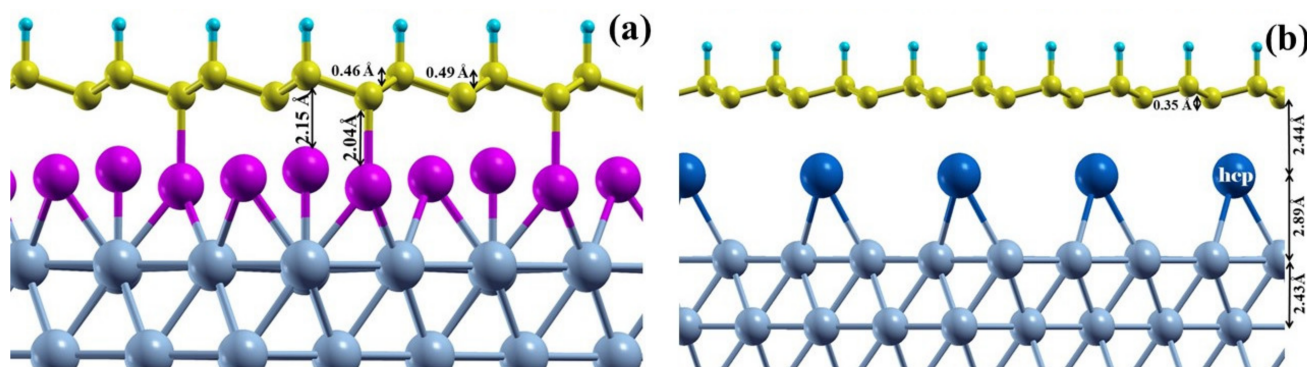


Figure 5. (a) Side view of Ni(111)/Al/GrH, (b) side view of Ni(111)/Na/GrH, where the atoms in cyan denote hydrogen.

Consistent with the geometry, we observe stronger Ni–Al and Al–C interactions in Ni(111)/Al/GrH than in Ni(111)/Al or Ni(111)/Al/Gr. Consequently, we observe the following changes in the magnetic moments on the atoms at the interface: the magnetic moment on Ni¹ decreases from 0.36 μ_B to 0.21 μ_B , while, for the remaining three surface Ni atoms, a reduction of about 0.15 μ_B could be observed. The magnetic moment on unhydrogenated C in graphone is almost completely quenched. Thus, the ferromagnetic graphone (in freestanding condition) becomes non-magnetic when supported on Ni(111)/Al substrate.

In the case of Ni(111)/Na/GrH, the hydrogenation of graphene favors a stable configuration at the fcc C of the graphone sheet, as shown in Figure 5b; the distance between Na and C is 2.44 Å. Unlike Al, there is no direct interaction of Na with C. The Ni–Na bond length is 2.89 Å. This shows that Na interacts feebly with the surface Ni atoms. After hydrogenation, there is a smaller buckling of about 0.35 Å compared to the Ni/Al/GrH configuration. The small amount of buckling arises due to the hydrogen adsorption, since graphone interacts weakly with the Na at the hcp site.

Unlike Ni(111)/Al/GrH, Ni(111)/Na/GrH shows many interesting magnetic properties. The magnetic moments of the surface Ni change upon interaction with Na from 0.71 μ_B (in clean Ni(111)) to 0.66 μ_B , while upon interaction with Na, a magnetic moment of around 0.63 μ_B can be observed. The unhydrogenated C, which interacts with (does not interact) Na, shows a magnetic moment of approximately 0.42 μ_B , which is aligned antiparallel (parallel) with respect to those on surface Ni atoms. Thus, the net magnetic moment on a graphone sheet is around 0.11 μ_B per C. This magnetic moment is lower by one order of magnitude than that found in freestanding graphone. However, it is greater by almost one order of magnitude than that observed in graphone supported on the Ni(111) surface.

4. Discussions

At the Ni(111)/graphone interface, the strong interaction between surface Ni and unhydrogenated C completely quenches the magnetic moment of graphone, from 1 μ_B to 0.02 μ_B . Additionally, the magnetic moments on the surface Ni atoms decrease significantly, from 0.71 μ_B to 0.16 μ_B . Thus, the interface formed with two strong ferromagnetic surfaces, Ni(111) and graphone, fails to show good potential for spintronic device applications with weak interfacial magnetic properties. Hence, in this study, we tried to alter the properties at the Ni(111)/GrH interface by intercalating Al and Na atoms.

With Al intercalation, it can be observed that Al interacts with surface Ni and unhydrogenated C atoms (Figure 6). The interaction at the interface is such that more spin-up states become unoccupied for surface Ni atoms. This reduces the spin polarization; hence, the magnetic moment on surface Ni is significantly reduced, from 0.71 μ_B on clean Ni(111) surface to 0.17 μ_B in Ni(111)/Al/GrH. Moreover, the magnetic moment on GrH is also almost completely quenched. Thus, like Ni(111)/graphone, the Ni(111)/Al/graphone interface shows weak interfacial properties.

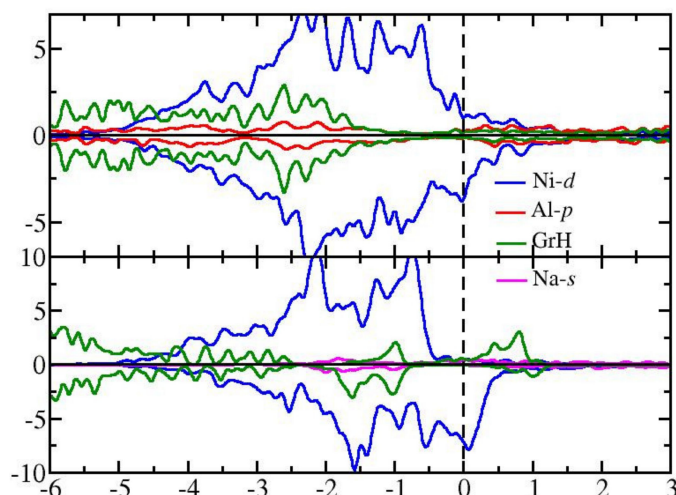


Figure 6. The density of states projected in the upper panel represents the intercalated configuration of Al with graphone, blue—d states of Ni/Al/GrH; the lower panel represents the intercalated configuration of Na with graphone, Ni/Na/GrH, blue—Ni d states, green—the sum of states for GrH, red—p states of Al, pink—s states of Na.

At the Ni(111)/Na/GrH interface, Na interacts relatively more strongly with unhydrogenated C than with surface Ni. As a result, only small changes are observed in the electronic and magnetic properties of surface Ni. From the DOS plot in Figure 6, the Ni-d state exhibits half-metallic behavior similar to that of clean Ni(111) surfaces. Additionally, the magnetic moment on the surface Ni atoms decreases slightly from $0.71 \mu_B$ on the clean Ni(111) surface to $0.64 \mu_B$ in Ni(111)/Na/GrH. The magnetic moment on GrH is quenched ($0.11 \mu_B$) compared to that in freestanding graphone ($1 \mu_B$). However, they are almost one order of magnitude greater than that at the Ni(111)/GrH interface ($0.02 \mu_B$).

5. Conclusions

To achieve a better understanding of the tuning of semi-metallic graphene properties, we studied the semi-hydrogenation of graphene sheets to form graphone. The transformation was studied by supporting graphone on a Ni(111) surface, due to their approximate closeness in terms of lattice parameter matching. In order to tune the magnetic and electronic properties at the interface between graphone and metal surfaces, the present DFT investigations employed the intercalation of Al and Na atoms. On the basis of our calculations, we observed that the interaction of Al with the surface Ni atoms was more vital than that of Na, which was feeble. This was evident from the difference in the magnetic moments observed in the absence and presence of graphone when Al and Na atoms were adsorbed onto the Ni(111) surface. This difference in the interaction at the Ni(111)/GrH interface when the Al and Na atoms were intercalated results in different interfacial properties. Of the two, Ni(111)/Na/GrH shows better magnetic properties from the point of view of spintronic device applications.

Thus, the intercalation of atoms between Ni(111) and graphone plays a significant role in tuning interface properties, such that the unique properties can find appropriate use as spintronic or semiconducting materials in the development of smart devices.

Author Contributions: R.A.: Conceptualization of the research idea, performing calculations, formal analysis and interpretation, drafting of the manuscript. N.J.: Formal analysis and interpretation of the investigations, drafting of the manuscript. These authors (R.A. and N.J.) contributed equally to the current research investigation. T.R.: Project supervision, reviewing and editing of the manuscript. All authors have read and agreed to the published version of the manuscript.

Funding: This research received no external funding.

Acknowledgments: It is a privilege for the authors to acknowledge CSIR—National Chemical Laboratory, Pune, India for providing the opportunity and facilities necessary to carry out this research work. The calculations were carried out using the 4PI cluster at CSIR—Centre for Mathematical Modeling and Computer Simulation (CMMACS), Bangalore, India, whom the authors thank for providing the HPC facilities. We also would like to acknowledge Hemant Darbari (Director General) Centre for Development of Advance Computing (CDAC)-Pune for providing the PARAM-Brahma HPC facilities as some of the calculations were performed by availing this facility.

Conflicts of Interest: The authors declare no conflict of interest.

References

1. Geim, A.K.; Novoselov, K.S. The rise of graphene. *Nat. Mater.* **2007**, *6*, 183–191. [[CrossRef](#)] [[PubMed](#)]
2. Englert, J.M.; Dotzer, C.; Yang, G.; Schmid, M.; Papp, C.; Gottfried, J.M.; Steinrück, H.P.; Spiecker, E.; Hauke, F.; Hirsch, A. Covalent bulk functionalization of graphene. *Nat. Chem.* **2011**, *3*, 279–286. [[CrossRef](#)] [[PubMed](#)]
3. Brzhezinskaya, M.; Kononenko, O.; Matveev, V.; Zotov, A.; Khodos, I.I.; Levashov, V.; Volkov, V.; Bozhko, S.I.; Chekmazov, S.V.; Roshchupkin, D. Engineering of Numerous Moiré Superlattices in Twisted Multilayer Graphene for Twistronics and Straintronics Applications. *ACS Nano* **2021**, *15*, 12358–12366. [[CrossRef](#)] [[PubMed](#)]
4. Georgakilas, V.; Otyepka, M.; Bourlinos, A.B.; Chandra, V.; Kim, N.; Kemp, K.C.; Hobza, P.; Zboril, R.; Kim, K.S. Functionalization of Graphene: Covalent and Non-Covalent Approaches, Derivatives and Applications. *Chem. Rev.* **2012**, *112*, 6156–6214. [[CrossRef](#)]
5. Sofo, J.O.; Chaudhari, A.S.; Barber, G.D. Graphane: A two-dimensional hydrocarbon. *Phys. Rev. B Condens. Matter. Mater. Phys.* **2007**, *75*, 153401. [[CrossRef](#)]
6. Shnitov, V.V.; Rabchinskii, M.K.; Brzhezinskaya, M.; Stolyarova, D.Y.; Pavlov, S.V.; Baidakova, M.V.; Shvidchenko, A.V.; Kislenko, V.A.; Kislenko, S.A.; Brunkov, P.N. Valence Band Structure Engineering in Graphene Derivatives. *Small* **2021**, *17*, 2104316. [[CrossRef](#)]
7. ZZhang, W.; Lu, W.-C.; Zhang, H.-X.; Ho, K.; Wang, C. Hydrogen adatom interaction on graphene: A first-principles study. *Carbon* **2018**, *131*, 137–141. [[CrossRef](#)]
8. Brzhezinskaya, M.; Shmatko, V.; Yalovega, G.; Krestinin, A.; Bashkin, I.; Bogoslavskaja, E. Electronic Structure of Hydrogenated Carbon Nanotubes Studied by Core Level Spectroscopy. *J. Electron. Spectrosc. Relat. Phenom.* **2014**, *196*, 99. [[CrossRef](#)]
9. Zhou, J.; Wang, Q.; Sun, Q.; Chen, X.S.; Kawazoe, Y.; Jena, P. Ferromagnetism in semihydrogenated graphene sheet. *Nano Lett.* **2009**, *9*, 3867–3870. [[CrossRef](#)]
10. Feng, L.; Zhang, W.X. The structure and magnetism of graphone. *AIP Adv.* **2012**, *2*, 042138. [[CrossRef](#)]
11. Šljivančanin, Ž.; Balog, R.; Hornekær, L. Magnetism in graphene induced by hydrogen adsorbates. *Chem. Phys. Lett.* **2012**, *541*, 70–74. [[CrossRef](#)]
12. Brzhezinskaya, M.; Belenkov, E.A.; Greshnyakov, V.A.; Yalovega, G.E.; Bashkin, I.O. New aspects in the study of carbon-hydrogen interaction in hydrogenated carbon nanotubes for energy storage applications. *J. Alloys Compd.* **2019**, *792*, 713–720. [[CrossRef](#)]
13. Morse, J.R.; Zugell, D.A.; Patterson, E.; Baldwin, J.W.; Willauer, H.D. Hydrogenated graphene: Important material properties regarding its application for hydrogen storage. *J. of Power Sources* **2021**, *494*, 229734. [[CrossRef](#)]
14. Zhao, W.; Gebhardt, J.; Späth, F.; Gotterbarm, K.; Gleichweit, C.; Steinrück, H.P.; Görling, A.; Papp, C. Reversible hydrogenation of graphene on Ni(111)-synthesis of graphone. *Chem.—Eur. J.* **2015**, *21*, 3347–3358. [[CrossRef](#)]
15. Sutter, P.; Sadowski, J.T.; Sutter, E.A. Chemistry under cover: Tuning metal-graphene interaction by reactive intercalation. *J. Am. Chem. Soc.* **2010**, *132*, 8175–8179. [[CrossRef](#)]
16. Pervan, P.; Lazić, P. Adsorbed or intercalated: Na on graphene/Ir(111). *Phys. Rev. Mater.* **2017**, *1*, 044202. [[CrossRef](#)]
17. Karpan, V.M.; Khomyakov, P.A.; Starikov, A.A.; Giovannetti, G.; Zwierzycki, M.; Talanana, M.; Brocks, G.; Van Den Brink, J.; Kelly, P.J. Theoretical prediction of perfect spin filtering at interfaces between close-packed surfaces of Ni or Co and graphite or graphene. *Phys. Rev. B* **2008**, *78*, 195419. [[CrossRef](#)]
18. Halle, J.; Néel, N.; Kröger, J. Filling the Gap: Li-Intercalated Graphene on Ir(111). *J. Phys. Chem. C* **2016**, *120*, 5067–5073. [[CrossRef](#)]
19. Weser, M.; Voloshina, E.N.; Horn, K.; Dedkov, Y.S. Electronic structure and magnetic properties of the graphene/Fe/Ni(111) intercalation-like system. *Phys. Chem. Chem. Phys.* **2011**, *13*, 7534–7539. [[CrossRef](#)]
20. Praveen, C.S.; Piccinin, S.; Fabris, S. Adsorption of alkali adatoms on graphene supported by the Au/Ni(111) surface. *Phys. Rev. B Condens. Matter Mater. Phys.* **2015**, *92*, 075403. [[CrossRef](#)]
21. Joshi, N.; Gaurav, C.; Ballav, N.; Ghosh, P. Tuning electronic and magnetic properties of the graphone/Ni(111) interface by oxygen intercalation: A first-principles prediction. *Phys. Rev. B* **2020**, *101*, 195401. [[CrossRef](#)]
22. Giannozzi, P.; Baroni, S.; Bonini, N. QUANTUM ESPRESSO: A modular and open-source software project for quantum simulations of materials. *J. Phys. Condens. Matter.* **2009**, *21*, 395502. [[CrossRef](#)] [[PubMed](#)]
23. Vanderbilt, D. Communications Soft self-consistent pseudopotentials in a generalized eigenvalue formalism. *Phys. Rev. B* **1990**, *41*, 7892–7895. [[CrossRef](#)] [[PubMed](#)]
24. Perdew, J.P.; Burke, K.; Ernzerhof, M. Generalized Gradient Approximation Made Simple. *Phys. Rev. Lett.* **1996**, *77*, 3865–3868. [[CrossRef](#)]
25. Monkhorst, H.J.; Pack, J.D. Special points for Brillouin-zone integrations. *Phys. Rev. B* **1976**, *13*, 5188–5192. [[CrossRef](#)]

-
26. Marzari, N.; Vanderbilt, D.; de Vita, A.; Payne, M.C. Thermal Contraction and Disorder of the Al(110) Surface. *Phys. Rev. Lett.* **1999**, *82*, 3296–3299. [[CrossRef](#)]
 27. Park, Y.S.; Park, J.H.; Hwang, H.N.; Laishram, T.S.; Kim, K.S.; Kang, M.H.; Hwang, C.C. Quasi-free-standing graphene monolayer on a Ni crystal through spontaneous Na intercalation. *Phys. Rev. X* **2014**, *4*, 031016. [[CrossRef](#)]
 28. Voloshina, E.N.; Generalov, A.; Weser, M.; Böttcher, S.; Horn, K.; Dedkov, Y.S. Structural and electronic properties of the graphene/Al/Ni(111) intercalation system. *New. J. Phys.* **2011**, *13*, 113028. [[CrossRef](#)]